Tanase, M.A. et al. (2019) 'Synthetic aperture radar sensitivity to forest changes: A simulations-based study for the Romanian forests', The Science of the total environment, 689, pp. 1104–1114.

Available at http://dx.doi.org/10.1016/j.scitotenv.2019.06.494

(Article begins on next page)

Synthetic Aperture Radar sensitivity to forest changes: a simulations-based study for the Romanian forests

Mihai A. Tanase[1,3],*, Ludovic Villard[2], Diana Pitar[1], Bogdan Apostol[1], Marius Petrila[1], Serban Chivulescu[1], Stefan Leca[1], Ignacio Borlaf Mena[1], Ionut-Silviu Pascu[1,5], Alexandru-Claudiu Dobre[1,5], Daniel Pitar[1], Gheorghe Guiman[1], Adrian Lorent[1,5], Cristian Anghelus[1], Albert Ciceu[1], Gabriel Nedea[1], Raducu Stanculeanu[1], Flaviu Popescu[1], Cristina Aponte[4], and Ovidiu Badea[1,5]

[1] National Institute for Research and Development in Forestry "Marin Dracea", 128 Blvd. Eroilor, Voluntari 077190, Ilfov, Romania

[2] Center for the Study of the Biosphere from Space (UMR CNES-CNRS-IRD-UPS), 18 av. Edouard Belin, Toulouse 2801, France

[3] Department of Geology, Geography and the Environment, University of Alcala, c/ Colegios 2, 28801 Alcala de Henares, Spain

[4] School of Ecosystem and Forest Sciences, University of Melbourne, 500 Yarra Boulevard, Richmond, Victoria 3121, Australia

[5] Faculty of Silviculture and Forest Engineering, "Transilvania" University of Brașov, 1 Șirul Beethoven, 500123, Romania

* Corresponding author

Abstract

Natural and anthropogenic disturbances pose a significant threat to forest condition. Continuous, reliable and accurate forest monitoring systems are needed to provide early warning of potential declines in forest condition. To address that need, state-of-the-art simulations models were used to evaluate the utility of C-, L- and P-band synthetic aperture radar (SAR) sensors within an integrated Earth-Observation monitoring system for beech, oak and coniferous forests in Romania.

The electromagnetic simulations showed differentiated sensitivity to vegetation water content, leaf area index, and forest disturbance depending on SAR wavelength and forest structure. C-band data was largely influenced by foliage volume and therefore may be useful for monitoring defoliation. Changes in water content modulated the C-band signal by less than 1 dB which may be insufficient for a meaningful retrieval of drought effects on forest. C-band sensitivity to significant clear-cuts was rather low (1.5 dB). More subtle effects such as selective logging or thinning may not be easily detected using C- or L-band data with the longer P-band needed for retrieving small intensity forest disturbances. Overall, the simulations emphasize that additional effort is needed to overcome current limitations arising from the use of a single frequency, acquisition time and geometry by tapping the advantages of dense time series, and by combining acquisitions from active and passive sensors. The simulation results may be applicable to forests outside of Romania since the forests types used in the study have similar morphological characteristics to forests elsewhere in Europe.

Keywords: forest monitoring, synthetic aperture radar, microwave simulations, MIPERS^{4D}

1. Introduction

Terrestrial ecosystems provide essential services to human societies (Daily, 1997). Forests are among the most biodiverse terrestrial ecosystems, provide habitat for a wide range of species, are a key element for carbon sequestration, are a major component of rural development, provide protective functions for soil, water and infrastructure, and contribute goods and services (Ojea et al., 2010). Sustainable forest management is needed for forests to continue providing such services (Obersteiner et al., 2010; Schaich and Milad, 2013).

Environmental and anthropogenic disturbances pose a threat to the function of forest ecosystems, leading to habitat degradation, increased risk of collapse, and loss of forest services (Michel and Seidling, 2014). Climate change will have further effects on terrestrial biomes, particularly forests (Saxe et al., 2001). Rising temperatures and falling annual precipitation in numerous regions has accelerated over the past decades affecting both local (Jenkins et al., 2000) and broad-scale ecosystem processes, including disturbance regimes (Dale et al., 2001).

The importance of forest ecosystems is highlighted by the many regional and global programs aimed at evaluating, monitoring, and reporting on forest condition, such as the International Co-operative Programme (ICP) on Assessment and Monitoring of Air Pollution Effects on Forests (ICP-Forests) operating under the United Nations (UN) Economic Commission for Europe (ECE) Convention on Long-range Transboundary Air Pollution (CLRTAP), the UN Collaborative Programme on Reducing Emissions from Deforestation and Forest Degradation (REDD), the International Long Term Ecological Research Network (ILTER), the Japan Aerospace Exploration Agency (JAXA) Kyoto & Carbon (KC) Initiative, the NASA`s Carbon Monitoring System (CMS), the European Space Agency (ESA) Climate Change Initiative (CCI) as well as countless national programs focused on forest health monitoring and forest inventory. Such programs use an array of data sources including *in situ* measurements, sensor networks, and information acquired by aerial and satellite earth observation (EO) platforms. EO datasets may be acquired by a range of sensors. Active sensors (e.g., radar, lidar) emit energy and measure the returns reaching the sensor from targets on the ground. Passive sensors (e.g. optic, thermal) detect radiation emitted from other source (e.g. sun, earth). Optical remote sensing is commonly used for monitoring forests due to intuitive interpretation, the wide range of spatial and temporal resolutions, and the long-time data series available from space-borne platforms. However, optical sensors have limitations in areas with frequent cloud cover (e.g. tropics) and low solar illumination angles (e.g. arctic) (Verbyla et al., 2008). In addition, optical sensors often fail to produce accurate results due to factors such as sensitivity to forest cover rather than structure and plant phenology (Tanase et al., 2011a). The use of active sensors may overcome such limitations given their independence of cloud cover and solar illumination, day and night acquisition opportunities and their ability to provide a direct measure of vegetation structure (Le Toan et al., 1992; Lewis and Henderson, 1999). Modern synthetic aperture radar (SAR) systems can measure both the backscatter coefficient, related to target scattering properties, and the scattering phase, related to the distance between the sensor and the target. In forestry applications the phase information is often used to derive forest height through interferometric (InSAR) processing (Askne et al., 2003; Garestier et al., 2008; Tanase et al., 2015a).

In the last three decades, the use of EO-derived data expanded prodigiously encompassing most areas of forest information needs including forest disturbance (Mermoz and Le Toan, 2016; Solberg et al., 2013; Tanase et al., 2015a), species and habitats (Laurin et al., 2016; Zhao et al., 2018), forest structure (García-Martín et al., 2008; Lange and Solberg, 2008; Lucas et al., 2010; Santoro et al., 2012; Solberg, 2010) and biomass (Karlson et al., 2015; Mitchard et al., 2011b; Neumann et al., 2012; Sandberg et al., 2011; Tanase et al., 2014), carbon budgets (DeFries et al., 2007 ; Lohberger et al., 2017; McNicol et al., 2018; Mitchard, 2018; Poulter et al., 2015; Seidl et al., 2014), forest health (Rullan-Silva et al., 2013; Spruce et al., 2011) and forest regrowth (Tanase et al., 2011b), as well as impact assessment of biotic (e.g. pests) and abiotic (e.g. fire, wind) natural hazards (Nielsen et al., 2014; Senf et al., 2017; Tanase et al., 2018; Tanase et al., 2015b). Most studies focused on local to regional levels but information on a limited range of parameters is available over wider areas from a range of projects (Baccini et al., 2008; Hansen et al., 2013; Hansen et al., 2003; Lefsky, 2010; Saatchi et al., 2011; Shimada et al., 2014; Simard et al., 2011; Tanase et al., 2015b). Nevertheless, products generated at continental to global scales are of limited use for national forest policies and management decisions due to diverse factors: i) low temporal frequency (e.g., one off, multi-annual), ii) generally low (100-1000m) spatial resolutions and forest heterogeneity, iii) unknown errors at national levels, iv) compromises in the retrieval algorithms which need to account for a wide range of conditions (e.g., boreal to tropical) and, v) the lack of calibration data over large tracts of forests (i.e. in situ data for algorithm development is sourced from relatively few countries). Indeed, some studies have shown large differences between global products specified accuracy and in situ samples at national to regional scales (Michelakis et al., 2014; Mitchard et al., 2011a; Rodríguez-Veiga et al., 2016; Tropek et al., 2018) with locally developed products providing significant increases of forest parameters estimation accuracy (Michelakis et al., 2014; Rodríguez-Veiga et al., 2016). Furthermore, locally developed products are needed when the forest parameters of interest are not available from globally-derived datasets or have inadequate temporal sampling or spatial resolution.

Romanian forests are under pressure due to a changing climate (increased aridity), natural disturbances (e.g., windthrows, insect outbreaks, fire) and anthropogenic factors related to management practices and clearing activities which affect ecosystem processes and biodiversity (Anfodillo et al., 2008; Gazol et al., 2015; Popa, 2008; Scheller and Mladenoff, 2005; Schimel et al., 2000). Indeed, monitoring activities based on remote sensing data suggest that high rates of forest disturbance in Romania were related to socio-economic changes

(Knorn et al., 2012). Furthermore, increasing natural disturbances caused by climatic variations create additional strains on forest ecosystems. Therefore, a continuous, reliable, and accurate national forest monitoring system is needed to provide early warning on forest condition by tracking natural and anthropogenic disturbances. Such monitoring systems may rely on information provided by field-based monitoring networks, in situ measurements, active and passive EO datasets, or by a hybrid approach. Past active (i.e. SAR) missions provided data with low temporal resolution which hindered the development of efficient forest monitoring algorithms. In addition, the utility of past sensors was limited by the available polarizations, steep viewing geometries and data access restrictions. With the launch of Sentinel-1 satellite constellation and the Advanced Land Observing Satellite Phased Array type L-band Synthetic Aperture Radar 2 (ALOS PALSAR-2) such limitations have been largely reduced. Sentinel-1, with high temporal resolution (images every three days) and improved sensor characteristics (e.g., dual polarization, increased spatial resolution and incidence angle, precise orbital information) presents new opportunities for the integration of SAR dataset into operational forest monitoring. Several variables may be relevant for forest monitoring for management, policy enforcement or national reporting purposes. However, only few such variables may be readily retrieved using EO data given the complexity of the interaction between land surface properties and the satellite's sensors. Our aim in this study was to assess, through state-of-the-art simulation models, the ability of SAR sensors to monitor the condition of Romanian forests. We hypothesised that currently available SAR sensors would be sensitive to changes in forest structural parameters and that such sensitivity could be used for improving operational forest monitoring systems. Specifically, our objectives were to i) describe the experimental setup and the field datasets used to constrain the SAR simulations and ii) asses the influence of changes in vegetation water content (VWC), leaf area index (LAI) and disturbance scenarios (e.g., defoliation, thinning, selective logging) on the C-, L-, and P-band SAR signal and thus the opportunity of monitoring forest condition and anthropogenic influences.

2. Material and methods

2.1 Study area

To evaluate the influence of forest vegetation properties on radar scattering, 24 one-hectare permanent sampling areas (PSA) were established within the EO-ROFORMON project in the meridional Carpathian range (Fig. 1A).

The meridional Carpathian range includes some of the highest mountain peaks as well as four of the six ecoregions present within the Romanian national territory (Olson et al., 2001). The PSAs fall within the forest districts of Mihesti, Musetesti, and Vidraru and include the four main forest types (oaks, beech, coniferous, and mixed) in Romania (Fig. 1B). The EO-ROFORMON permanent sampling network was established to monitor fast changing (e.g. defoliation, vegetation water content) as well as slow changing (e.g. height, dimeter at breast height) forest parameters.

The Experimental Forest District (EFD) Mihaesti was one of the first places in Romania where experimental research programs were introduced (1892). The area is characterized by steep slopes and strong land fragmentation. The slopes are predominantly oriented towards south. Depending on altitude, the mean annual temperature is 8 to 10° C with mean annual precipitation around 760 mm. Precipitation is fairly distributed seasonally, with 100 to 150 mm being recorded during winters and autumns and around 200 mm being recorded during spring and summers. Maximum rainfall is recorded in June and minimum in February. The dominant winds blow from the west but windthrows are rare, with significant events being recorded only in 1961 and 2006. Soil types and subtypes are strongly depend on geomorphology, position on slope, slope orientation and forest type. Being relatively uniform within the EFD, the climatic and geological conditions have weak influence on soil diversity. The forest districts Musetesti and Vidraru are characterized by steep slopes oriented predominantly towards west and south-west, and respectively south and south-west. The mean annual temperature varies between 3.7°C and 6.1°C with mean annual precipitation between 860 and 1050 mm. The maximum rainfall is recorded in June and minimum in February.

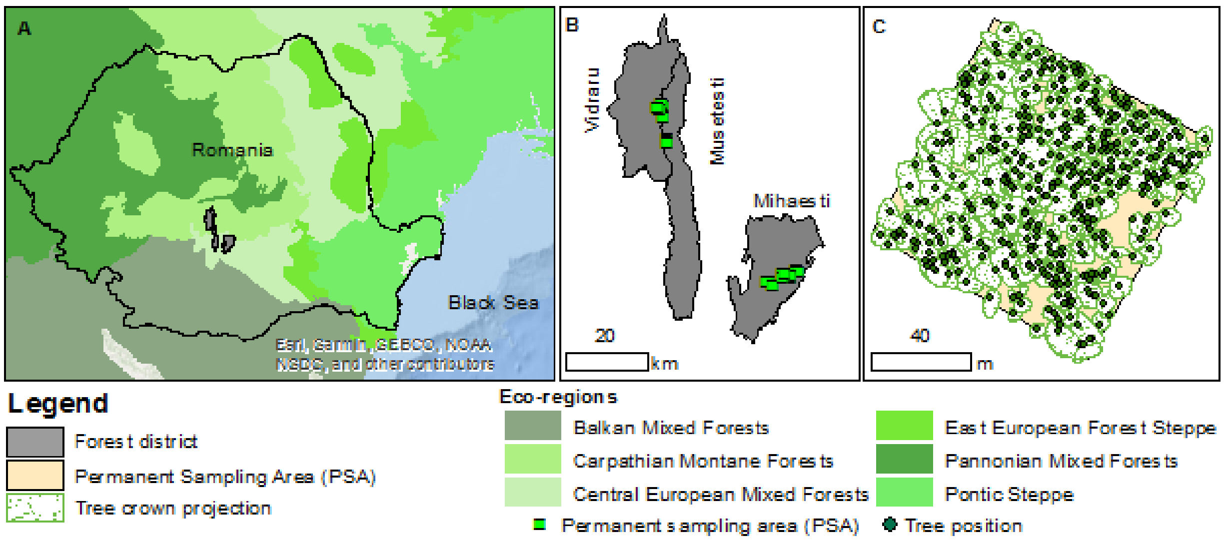

Fig. 1 Study area and the location of field sampling sites.

2.2 Field datasets

The in situ measurements, used to constrain the radar scattering simulations, were available from the EO-ROFORMON project. Field data collection aimed to characterise slow (e.g. species composition, tree height, forest volume) and fast (e.g., vegetation water content, leaf area index) changes in forest parameters which may result in large variations in radar scattering properties.

The PSAs, six for each forest type, were established within the forest district Mihaesti (oak and beech) and Musetesti/Vidraru (conifers and mixed forests). For each forest type, two PSAs constituted the reference (no silvicultural interventions) while four PSAs represented managed forests (i.e. two replicates for thinning and two for selective logging). The managed PSAs were selected in forest stands where interventions were planned between 2017 and 2019. The PSAs were clustered to facilitate access and minimize transport time. The reference PSAs were installed within the same forest stands as for the corresponding managed PSA thus minimizing differences (e.g., slope, orientation, species composition) between managed and reference samples. The PSAs were located close to access roads to reduce travel time but at least 50 m from the end of a forest stand. In each PSA, three clustered 500 m2 permanent sub-plots (PSP) were used for monitoring fast-changing forest parameters (i.e., LAI, foliage and trunk water content) on a monthly basis from April to October. Support measurements were also carried out to characterize environmental variables (e.g. volumetric soil moisture, temperature, and humidity) at the time of field sampling. Information related to species specific traits was

Table 1 List of parameters sampled at the continuous monitoring sites

Forest structure/inventory	Vegetation water content	Species traits	Other
Diameter at breast height	Foliage water content	Leaf	Soil moisture
Tree/crown height (selected PSAs)	Trunk water content	width/length	Temperature
Crown projection (selected PSAs)		weight (dry/wet)	Humidity
Understory (selected PSAs)		insertion angle	Tree growth
Leaf area index		radius	
		Primary / secondary branches	
		length /diameter	
		weight (dry/wet)	
		insertion angle	

collected (Table1) while ancillary sensors (i.e., soil moisture probes, girth bands, temperature and humidity sensors) were installed in the eight reference PSAs to avoid sensor damage by the planned silvicultural works. For eight PSAs, the slow changing forest parameters were recorded using computer assisted (i.e., FieldMap©) forest inventory methods (Hédl et al., 2009). For the remaining 16 PSAs the FieldMap© system was used at PSP level while classic inventory methods based on calipers and hypsometers were used to measure all the remaining trees. Through its integrated software/hardware solution, the FieldMap system records the precise XYZ coordinates for each tree together with, canopy height, crown projection, the position of coarse woody debris, and other attributes of interest such as understory and regeneration pockets (Fig. 1C). For increased productivity, tree heights were recorded with an ultrasonic Vertex hypsometer.

The fast-changing forest parameters were monitored through destructive sampling (foliage), terrestrial laser scanning (LAI) and contact sensors (trunk moisture, forest growth). Foliage sampling included the collection of leaves (or needles) from the upper part of the canopy in two representative trees for each tree species. Each sample was weighed in the field (fresh weight) using a portable balance and transported to the laboratory for dry weight measurement after being placed into an oven at 75^{0}C for 48 hours. Before drying, the foliage of each sample was spread on cardboard and a vertical photograph was taken using a fixed tripod and focal length. The photographs were used to determine the total leaf area for each sample (needed to compute water content per unit area) as well as species traits (e.g. mean and distribution of leaf/needle surface, perimeters, length, and diameter). After determining the dry weight, the samples collected at each PSP were combined (by tree species), grinded, and chemical analyses were carried out to determine the C and N content at each sampling date. Based on the wet and dry weight, the vegetation water content and the equivalent water thickness (EWT) were computed (eq.1 and eq. 2).

$$VWC = \frac{FreshWeight - DryWeight}{DryWeight} (kg\ kg^{-1}) \qquad (1)$$

$$EWT = \frac{FreshWeight - DryWeight}{Area} (kg\ m^{-2}) \qquad (2)$$

Temporal variations in canopy structure were determined using leaf area index (LAI) as a proxy. The LAI, computed at the center of each PSP, was based on digital canopy photography (Alivernini et al., 2018) by taking advantage of the photographs recorded by the digital camera incorporated into the TLS. The resulting panoramic images were re-projected and decomposed in six facets to analyze them as a ratio of large (inter-canopy) and small (intra-canopy) gaps. This allowed for corrections to be applied regarding leaf clumping and solar radiation extinction (Wang et al., 2007).

2.3 SAR signal simulation

The data collected at PSPs level were used to constrain the Multistatic Polarimetric Interferometric Electromagnetic model for Remote Sensing – MIPERS^{4D} (Villard, 2009) simulations assessing the extent to which fast changing parameters (e.g. MC, LAI) influence radar scattering properties. MIPERS^{4D} considers the key interactions (propagation and scattering phase) of individual dielectric elements (modelled as ellipsoids and cylinders) with the incoming microwaves by using a distorted Born approximation and an approximate solution of Maxwell's equations of the scattered medium. MIPERS^{4D} simulated observable and measurable remote sensing SAR datasets based on realistic scenes of natural vegetation parametrized using the detailed in situ datasets acquired at four PSAs. The MIPERS^{4D} model describes spatial heterogeneities by using homogeneous strata that can be overlaid vertically and arranged horizontally. Each layer is characterized by its extinction coefficient and different statistical options can be used to generate strata depending on the suitable probability distribution function (pdf). Therefore, the geometrical dimensions and orientation of scatterers may follow specific rules or can be driven by tree growth models. Ground contributions are modeled based on slope angles, roughness and local soil permittivity, and deterministic (caused by the travelling wave path) and random (reproduce the speckle effect) phase components (Villard et al., 2016). As inputs, MIPERS^{4D} used a precise digital terrain model (DTM) obtained from interpolating (triangular irregular network) the z coordinates of each FieldMap measured tree. Based on tree location, diameter at breast height (DBH), and height MIPERS^{4D}

generated PSA mockups characterized by near-real vegetation volume fraction when considering the use of species-specific tapering factors (as derived from the in situ data), allometric equations, tree species traits (i.e., leave/needles dimeter, length) and canopy volume (LAI). One should notice that in an inverse framework MIPERS^{4D} may be used to derive numerical invertible functions (NIFs) for retrieving the forest variables (FVs) of interest.

MIPERS^{4D} was also used to simulate the effect of vegetation removal on the SAR signal for forest stands (i.e., oak, beech, mixed forests) under different disturbance scenarios (defoliation, wind throws) and forest management objectives (thinning, selective logging). The aim to assess the opportunity offered by SAR time-series for monitoring forest condition and change due to anthropogenic factors. Thus, an important part of the experiment was assessing the interactions caused by simultaneous changes in canopy foliage, vegetation water content and forest logging. Given the current availability of spaceborne SAR data at L- and C-bands, and from soon to be launched ESA`s at P-band Biomass mission, a specific focus has been placed on these frequencies. Considering previous knowledge, three core parameters have been identified as having an important role in scattering temporal behavior, namely vegetation water content, leaf area index, and Forest Disturbance (FD). Indeed, these parameters concentrate several interests in forest monitoring and may impact significantly on the backscatter. In addition to the sensitivity analysis regarding these parameters the study took advantage of the simulation capabilities of MIPERS^{4D} to isolate the various components to the total signal (section 3.4).

3. Results

3.1 Forest structure and seasonal variability

The above ground volume (AGV) varied from 200 m3 in young oak stands to over 1000 m3 in old growth mixed (beech and Norway spruce) forests with average tree height ranging between 12 and 29 m and average dbh between 10 and 59 cm (Table 2). Notice that, for each forest type, low dbh and h values in Table 2 correspond to young stands (n=3) where thinning works are carried out while high values correspond to old growth stands where logging for timber is carried out. The opposite is true for the number of trees. The mean leaf/needle length, and width remained fairly constant through the vegetation season (Appendix A) with C and N concentrations being particularly stable through the year and between PSAs. The wood water content varied by

10-25%, depending on species, with low values observed towards the end of the vegetation season. A clear temporal pattern was not observed for canopy water content (i.e., EWT). EWT varied temporally (vegetation season) and spatially (PSA level)) as it depended not only on species traits but also on specific site conditions which are modulated by slope, orientation, substrate, and rainfall patterns.

LAI values were rather stable through the vegetation season for coniferous (Norway spruce) species while for deciduous species (oak and beech) decreasing LAI values were observed towards the end of the vegetation season (Appendix A). One should notice that, early (March - April) and late (October - November) periods were problematic to sample due to the presence of snow cover and freezing temperatures, respectively. The bulk of foliage was largely formed in May (i.e., first sampling days) while foliage shedding was incomplete in October (the last sampling days).

3.4. SAR signal simulations

Based on forest structural information (number of trees, species, dbh classes, tapering factor, height, leaf/needle dimensions, DTM) mockups for four PSAs (beech, oak, and mixed forests) were generated and used for the MIPERS^{4D} simulations (Fig. 2). Notice that since field data from coniferous forest were not ready until late in 2018 simulations for coniferous forest were not possible. However, results for mixed forests (beech and Norway spruce) provide some indications on SAR signal sensitivity for such forest types.

Table 2 Mean forest structural characteristics observed at the EO-ROFORMON sampling sites

Main species	No. of trees for young and old stands	Mean DBH range (cm)	Mean H range (m)	Mean AGV range (m3)
beech (n=6)	1309 / 425	12.9-24.5	17.6-26.3	383.7-622.1
oaks (n=6)	2853 / 559	10.0-58.8	12.6-28.6	202.5-652.4
mixed (n=6)	1658 / 679	16.7-29.0	18.3-21.7	571.6-766.4
coniferous (n=6)	1583 / 624	16.6-31.2	15.6-22.5	260.4-783.0

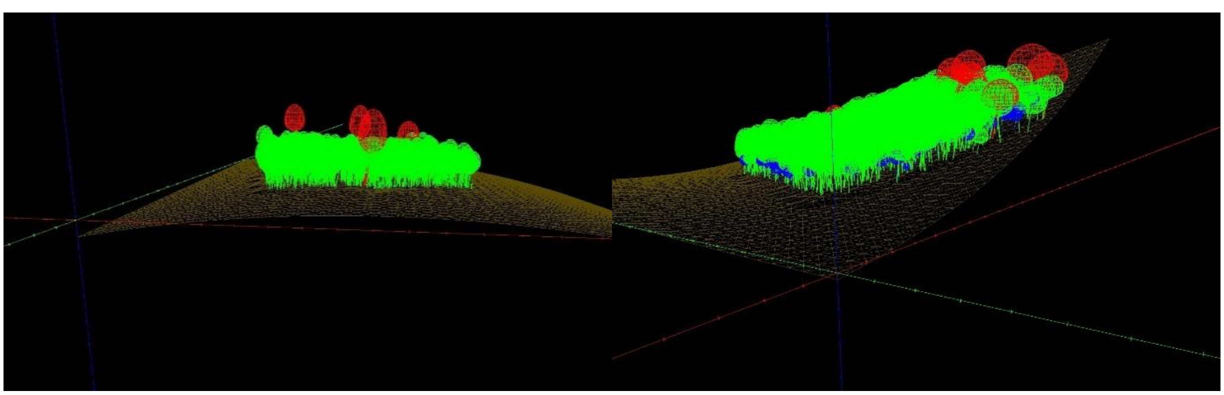

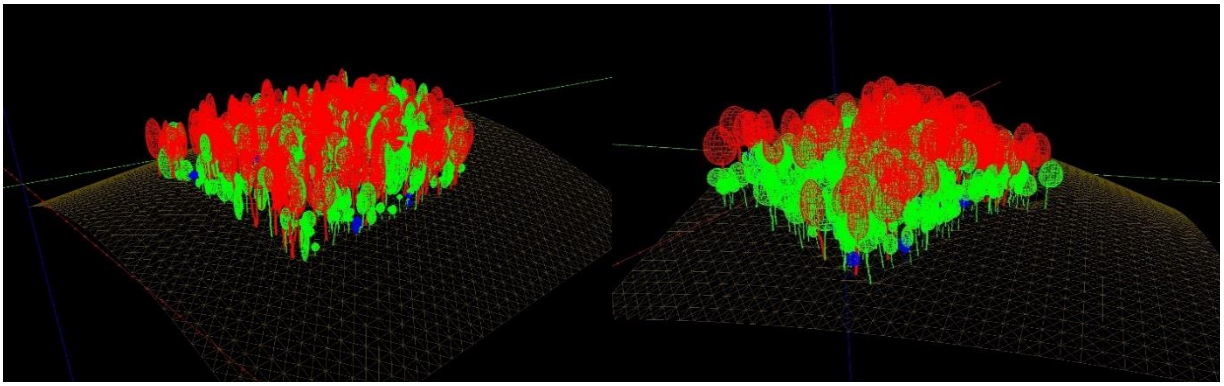

Fig. 2 Stand mockups used for MIPERS^{4D} simulations for young oak (Qu-Y, upper left), young beech (Fa-Y, upper right), old beech (Fa-O, lower left) and old mixed (Mix-O, lower right) forests. The red-green-blue colors represent three DBH classes (i.e., < 7.5 cm, 7.5-37.5 cm and >37.5 cm)

3.4.1 Backscattering components

MIPERS^{4D} made possible the extraction of various contributions which compose the total signal as measured from real sensors. Such capability is essential to better understand the underlying physics which govern the relation between radar backscatter and forest parameters of interest. For example, contributions due to branches and leaves (needles) may be clearly distinguished for each of the four PSA tested (Fig. 3, left panel). The balance between branch and leaves contributions varies according to forest structure with contributions from branches being mostly lower than ones from leaves, but higher than ones from needles. Such effects are more pronounced for the co-polarized (VV) channel. Notice that contributions from trunks and the ground (through direct or coupling mechanism) have not been displayed for C-band given too small values (below -25 dB for the trunks and their -40 dB from the ground). The weak contributions from leaves at P- and L- bands, makes a similar representation less meaningful for these frequencies. However, simulation of the interferometric phase center heights is of interest at such increased wavelengths (Fig. 3, right panel). Considering an interferometric ambiguity height of 50 m and a radar elevation angle of 35°, the resulting phase center for each PSA can be seen in Fig. 3 (right panel). As expected, phase centers increase from P to C-band and are close to the forest top canopy height for higher frequency C-band. Interestingly the non-linear behavior between the differences at P-, L- and C-bands with PSA which is determined by a different effective attenuation as a function of forest structure.

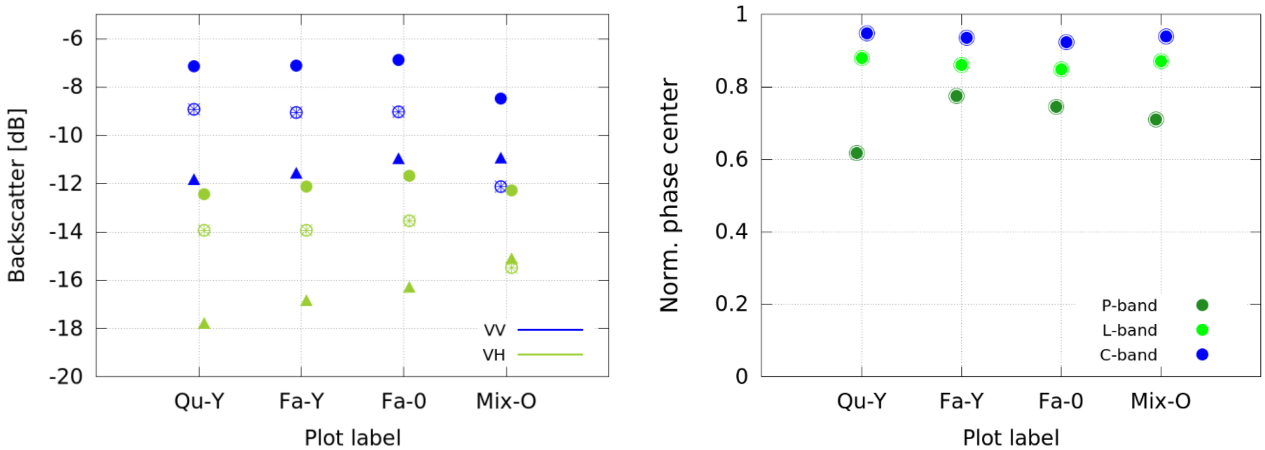

Fig. 3 Left panel: C-band VV (blue) and VH (green) backscattering coefficients with their respective decomposition between contributions from leaves or needles (cross-circle symbols) and branches. Right panel: Normalized interferometric phase center at P, L and C bands and for each of the forest test plot. Filled symbols represent the total backscatter contributions. The crossed-circles and the triangles represent leaves/needles and branches respectively (left panel only). Qu stands for sessile oak, Fa for beech and Mix for mixed coniferous and beech forests. Y stands for young and O stands for old growth forests.

3.4.2 Sensitivity to changes in vegetation water content

High contrast between the dielectric permittivity of water and that of dry vegetation matter suggests that temporal variations of water content may results in strong impacts on the complex permittivity of the scatterers (dielectric cylinders and ellipsoids) with the magnitude of change being comparable to that of a change of geometric dimensions (considering the effective wavelength) as detailed in Villard et al. (2016). However, changes in VWC also impact the extinction coefficient through the vegetation layers, with the total backscatter resulting from the opposite effects between increases of reflectivity at the scatter level and of attenuation at the bulk level. Electro-magnetic models are therefore relevant when assessing this combined effect, although the difficulty is in parametrizing VWC within the vegetation canopy. To that end, dielectric models have been derived considering previous research (McDonald et al., 2002) and recent experimental data during AfriScat and TowerScat campaigns (Hamadi et al., 2017). For the simulation scenarios, the reference considers a vertical gradient of VWC from 20 to 35% along the trunk, 35 to 45% for the branches and 50 to 60% for the leaves. A Gaussian distribution is considered with an error model (1-sigma) of 15%, which is further propagated into the MIPERS^{4D} model using a Monte-Carlo like process. According to this parameterization, backscattering coefficients varied as a function of VWC and the increasing wavelength from C- to P- bands (Fig. 4). As expected, C-band was less sensitive to VWC varying by less than 1dB between the different forest types and structures. The highest variation was observed for the P-band (about 7 dB) with beech stands varying by about 4 dB depending on age (young to old growth beech). At C-band, it is also worth noticing that the spread due to VWC is comparable to the spread from the considered forest types.

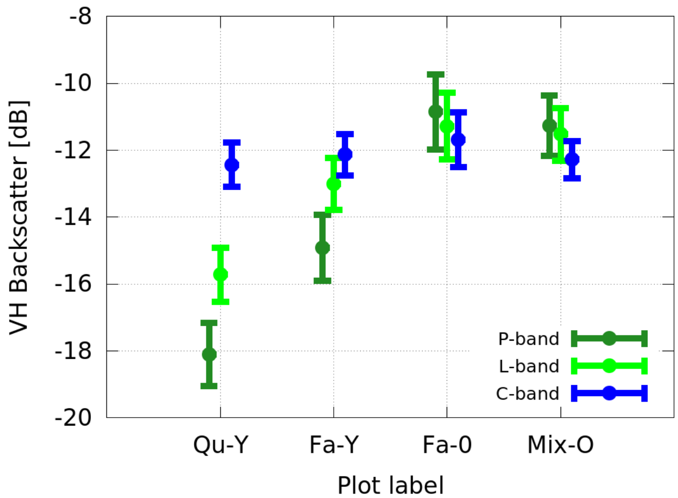

Fig. 4 Cross-polarized backscatter at C-, L- and P-band simulated for each PSA, with error bars indicating the possible dispersion (1-sigma) related to the VWC distributions detailed in the text. Qu stands for sessile oak, Fa for beech and Mix for mixed coniferous and beech forests. Y stands for young and O stands for old growth forests.

3.4.3 Sensitivity to changes in foliage

Foliage (estimated through LAI) is an important parameter which variations are closely linked to the environmental conditions as it is mostly driven by seasonal effects in the temperate eco-regions. Considering in situ LAI measurements from TLS data (PSP level), the LAI values have been extrapolated to PSA level with specific care on clumping factors and specificities due to the various forest species. The extrapolated LAI were used to parametrize the volume fraction of leaves, considering their mean geometrical dimensions derived from in situ measurements and completed with literature results (for leaf thickness). To assess a wider LAI variability which could be expected from longer experimental surveys, the values have been extrapolated from 0 to 5 m^2/m^2. The backscatter sensitivity analysis showed that C-band backscatter had the highest sensitivity to LAI (Fig. 5). However, one should also notice the significant decrease at L-band for the high range of LAI values, as well as the slight decreasing trend observed for the P-band. Further, a saddle shape was observed at C-band (both

VV and VH polarizations) reflecting the antagonist effects between the increasing reflectivity and attenuation. At C-band, similar saddle shapes were observed for all species, for both young and old forests (Fig. 6). The C-band sensitivity to LAI in the decreasing region (i.e. high LAI values) is lower for the VV polarization. Therefore, the ratio between VV and VH polarization is meaningful as it provides for a more straightforward relation with LAI than the standard backscattering coefficients which showed a quasi-monotonic trend rather than the saddle shape. Analyzing Figs 5 and 6, one may notice that the inversion point in the case of young beech forest is reached earlier than for older beech forest due to a lower effective attenuation caused by a more open forest structure for older forest.

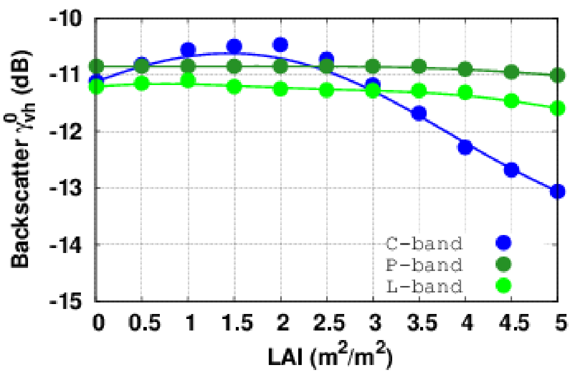

Fig. 5: VH backscattering coefficients at P- (green), L- (light green) and C-band (blue), as function of increasing LAI values for PSA SF10T (old beech forest)

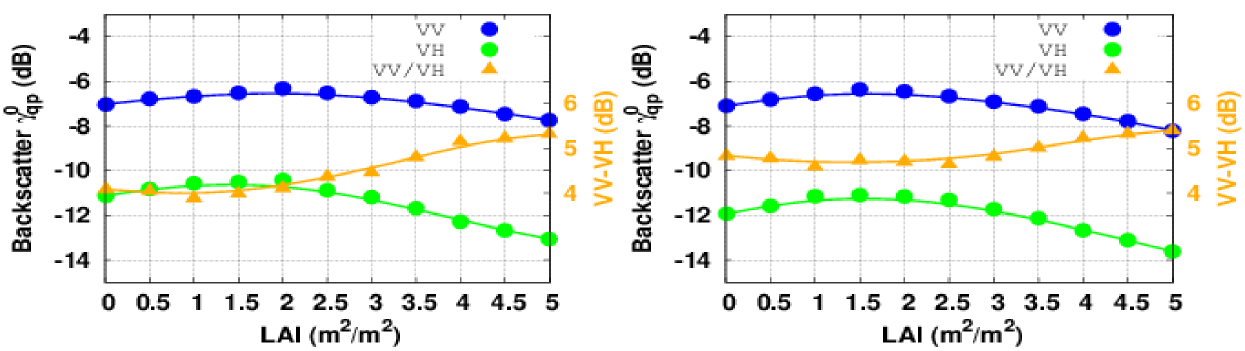

Fig. 6 C-band backscattering coefficients VV (blue) end VH (green) as function of LAI for old (Fa-O, left panel) and young (Fa-Y, right panel) beech forest. The ratio between VV and VH is indicated on the right axis.

3.4.4 Sensitivity to forest disturbance

Given the unprecedented time series of Sentinel-1 data (with revisit time up to 6 days), the impact of forest disturbances on C-band backscatter is of interest and raises questions regarding the many configurations that could be simulated. As a generic example (see left panel in Fig. 7), the case of a clear-cut in the middle of a homogeneous mature deciduous forest (25m mean height as per the descriptive parameters of PSA SF10T) was considered. The disturbed area was varied from 0 (reference) to a quarter hectare. The backscattering coefficient could be fairly estimated from experimental images considering the typical ground pixel spacing of Sentinel-1 (about 20m) and the need of spatial averaging to filter speckle effects. As expected, the lowest backscatter coefficient was observed over the shadowing region (with value far below ypical values NESZ of around -30 dB) while backscatter reinforcement (up to 3 dB at VV polarization and for a maximum soil moisture of 0.4 vol/vol) was observed at the front edge of the clearing. Considering these combined effects (shadowing and reinforcement), the average VV backscattering coefficient over 1 ha was not necessarily impacted by partial clear-cuts (Fig. 7, right panel). The change was less ambiguous for the VH polarization since the double bounce contribution, which mainly drives the reinforcement at the front -edge, is less important when compared to VV polarization.

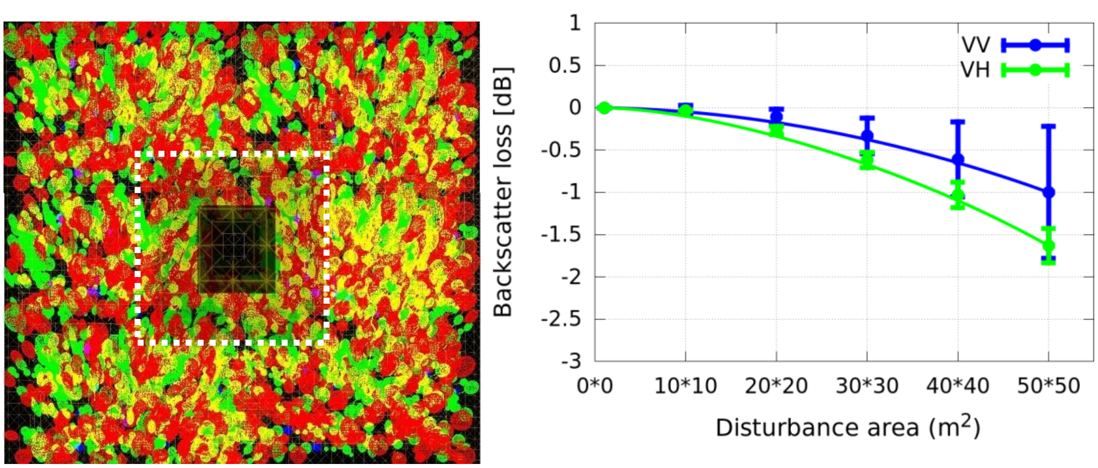

Fig. 7: Left image illustrates a 2D top view of a 50x50m disturbance (in black) within the1 ha forest plot (white delineation) located within a four-hectare stand (full simulated area). The impacts of several sizes of clear-cuts on the VV and VH backscattering coefficients are shown on the right, in which standard deviations (shown as error bars at 1 sigma) are due to variations in soil moisture, vegetation water content and leaf area index.

3.4.4 Sensitivity to combined changes due to VWC, LAI and logging

Based on the generic case detailed in above (3.4.3), additional effects of changes in VWC and LAI were considered on top of forest disturbance in stands affected by clear-cuts and selective logging. Considering the strong impact of topography and local geometry on backscatter (shadowing and layover effects) a titled or hilly ground below the forest may significantly bias the contrast between the ground contribution from deforested or intact areas. Therefore, for generalization, a generic forest (based on SF10T PSA data) over a flat terrain was hereafter considered. The backscatter change was computed as the averaged backscatter change for the 1 ha area. One should notice that for such scenarios, edge effects caused by inhomogeneities due to clear-cuts and the slant range radar geometry are spread on a wide zone, hence the need to simulate a much larger scene (4 ha) (as evident in Fig. 7). Since such simulations focus mainly on radar backscatter variations due to forest disturbance, the backscatter change in magnitude is here defined as the difference between the simulated perturbation minus the undisturbed one with the same LAI and VWC conditions, but repeated for all combinations of VWC and LAI at the origin of the displayed error bars.

C-band simulations for each polarization (VV and VH) were shown in Fig. 7 (right panel). For both polarizations, change was limited to 1.5 dB with much larger uncertainties on VV backscatter as soil moisture may obscure changes due to clear-cuts. For VH polarization, the change is less ambiguous. One should notice that upper bounds for LAI or VWC give the largest changes (lower values of backscatter due to higher attenuation). However, it is also important to notice that such changes in magnitude are about the same order (or less) when compared to those resulting from VWC or LAI variations. Considering the same scenario and metrics, the backscatter changes at L- and P-band have been simulated (Fig. 8 left panel). The results show stronger changes at P-band, while changes at L-band are still rather limited in comparison to those caused by variations due to VWC. As for the C-band (recalled in the same Figure), the apparent small backscatter loss is the result of opened areas creating an edge facing the radar which results in a strong backscatter enhancement (mainly due to coupling terms with the ground) that compensates the scattering volume loss.

Last, selective logging was simulated by extracting up to 10 individual trees with the biggest DBH (Fig. 8 right panel). While C-band was largely insensitive to this type of forest disturbance, the backscatter loss at P-

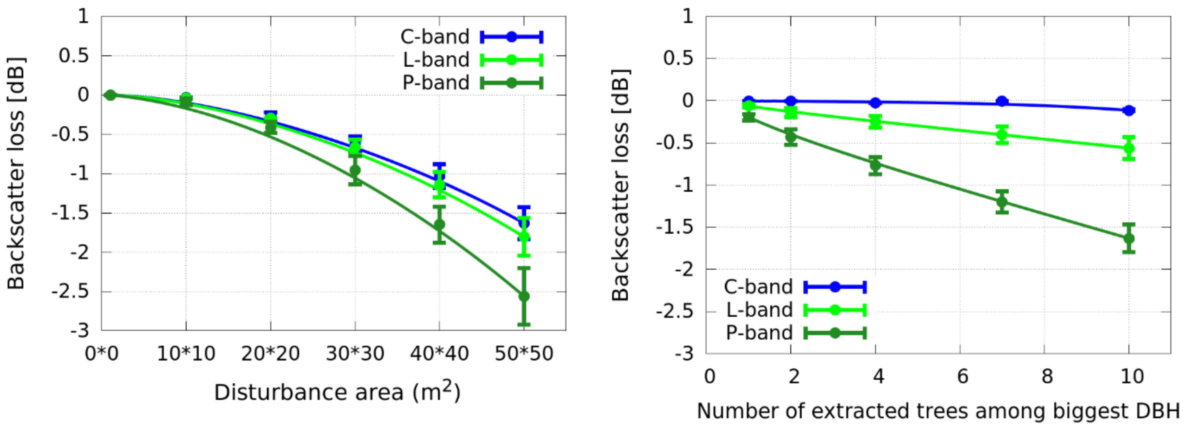

Fig. 8 Backscatter loss at C-, L-, and P-band for VH polarization as a function of clear-cut extent (left) and number of trees extracted (right). Error bars accounting for LAI and VWC uncertainties at 1-sigma.

band was significant. The uncertainties indicated by the error bars were mainly due to VWC changes (the LAI had a very small impact) which impact significantly the sensitivity to AGV. It is also important to notice that backscatter was derived from the difference with the non-disturbed case but with the same variation of VWC or LAI. Thus, these results can be compared to the specific sensitivity analysis detailed in the previous sections. Comparison shows that the maximum backscatter loss at L-band (for 10 extracted trees) might be misinterpreted with changes due to VWC variations. Such misinterpretation is however unlikely at P-band.

4. Discussion

Although forest monitoring from remote sensing data is scarce for Romanian forests, several studies have assessed the change in forest cover over the past decade (Griffiths et al., 2012; Knorn et al., 2012; Potapov et al., 2015). Such studies used optic imagery to estimate forest cover loss (defined as complete or nearly complete tree removal) and gain (areas where tree canopy cover reached a certain threshold by the end of the study period). Results from these studies suggest substantial changes in forest cover during the post-socialist period with timber harvesting being the main cause of forest loss followed by insect outbreaks and forest conversion (Potapov et al., 2015). Approximately 4.5% of Romanian forests were affected by at least one significant disturbance event (complete or nearly complete tree removal) over the past two decades. Non-state ownership regimes (i.e. private owners vs. public property) and species composition of restituted forests were two important factors determining disturbance and raised concerns regarding timber overexploitation in many areas (Griffiths et al., 2012). Such trends lead to an increasing loss of forest habitat, as well as more isolated and fragmented protected areas (Knorn et al., 2012). Therefore, a systematic forest monitoring system that differentiates between natural disturbances and logging activities is needed. Such a system may take advantage of the temporal dimension of changes in the remote sensing signal acquired by both passive (i.e. optical) and active (i.e. radar) sensors.

The ability to monitor forest changes from space depends on the sensitivity of the radiometric response to vegetation phenology and development stages. Increasing vegetation cover is readily detected by optical sensors up to the point of complete canopy cover. Past this point, changes in reflectance values largely relate to variations in other factors such as canopy water content, defoliation/discoloration. Tracking changes past canopy closure may be, however, achieved by integrating information from optical (i.e., cover related) and radar (volume related) sensors within a multi-temporal framework. To simulate, model, and validate EO-derived forest structural parameters in situ information is needed to drive and restrict the models to working within a valid range of conditions. Such ranges may be obtained by systematic measurements of parameters influencing the variability in the observed electromagnetic spectrum. Given the intensive labor and associated costs such measurements are only feasible over relatively small areas (hectares) and short time periods (years). The EO-ROFOMON project has established a permanent sampling network by responding to several key requirements: i) inclusion of the main Romanian forest types, ii) replicates for both young and old growth forests, iii) field monitoring of both fast and slow changing parameters with the highest influence on the EO data of interest and iv) in situ replicates for each forest type, age class, and silvicultural works..

The in situ monitoring activities showed that the selected PSAs were largely representative of the forest conditions in Romania. However, the beech PSAs represented a less diverse structure when compared to the Romanian national forest inventory (NFI) network for which beech dbh, height and AGV range between 6-91cm, 3-46 m and respectively 3-1450 m3. For the remaining species, the ranges were largely similar. However, one should notice that the NFI is carried out over much smaller plots (500 m2) which results in higher variability as small areas of very young or very old trees may influence mean values. Leaf and needle morphological characteristics were comparable with values recorded for the same species elsewhere. For European beech the observed mean and standard deviation for leaf area and length were slightly higher when compared with measurements observed at a range of sites (22.8 ±4.05 and respectively 6.59 ±7.2) in central Europe (Stojnić et al., 2016) while mean leaf width was largely the same (4.8 ±5.15) suggesting representativity of our in situ measurements, and thus of SAR simulation results, for a wider area. Similarly, the morphological characteristics observed for the sessile oak and Norway spruce were comparable with those encountered in other forests (Bruschi et al., 2003; Niinemets, 1997) as was the chemical composition (C and N) of needles (Niinemets, 1997) and beech and oak leaves (Bussotti et al., 2005; Petritan et al., 2010; Steffen et al., 2007). EWT values for oak and beech samples were also similar to those recorded elsewhere in Europe (Hill et al., 2011).

The LAI values observed for the sampled forests fall within the statistical distribution compiled for ttemperate deciduous broadleaf and needleleaf forests (Asner et al., 2003). For broadleaf deciduous forests, the mean and standard deviation observed for oak (3.9 ±0.6) and beech (4.6 ±1.0) were close to the mean global value for broadleaf deciduous forests (5.1 ±1.6). However, for coniferous stands the mean observed LAI value (12.7±4.4) was much larger when compared to the global mean for the temperate zone (5.5±3.4), being close to the upper limit (i.e., 15.0). The similarity of the observed value with those observed over many sites at global level (184 for deciduous broadleaf and 199 for evergreen needleleaf forest) provide some assurance on the adequacy of the DCP method used to compute the LAI values despite the lack of in situ measurements needed for a more rigorous accuracy estimation.

The electromagnetic simulations performed in this study enabled quantification of the strong difference in sensitivity to vegetation water content, leaf area index, and forest disturbance between P, L and C-bands for several forest types. At C-band, the contribution from leaves to the backscatter coefficient was higher for all stands when compared to the contribution from branches. Cross polarized backscatter at C-band was not influenced by stand structure or species. Conversely L- and P-band cross-polarized backscatter varied significantly with stand age suggesting the need for longer wavelengths when detecting changes in forests. Nevertheless, the C-band data was sensitive to foliage volume with increased attenuation being observed for LAI values above three (Fig 5). Due to increased contributions from leaves (Fig 3), C-band may provide opportunities to monitor changes due to defoliation for forests with moderate LAI values particularly when using the ratio between co- and cross-polarized channels as also demonstrated elsewhere (Salberg et al., 2009). Changes in water content modulated the C-band signal by less than 1 dB (Fig. 4) which may be insufficient for monitoring drought effects on forest condition. However, since severe drought is often associated with foliage loss forest condition monitoring using C-band is still possible, particularly when using the co- to cross-polarization ratio which provides for a more straightforward relationship with changes in canopy structure. One should notice that current and future L- and P-band SAR missions provide less frequent acquisitions when compared to the Sentinel-1 mission (3 days when both ascending and descending passes are used) and therebefore, their utility is severely limited within a such a monitoring context.

The analysis has also shown that the effects of significant perturbations (e.g. clear-cuts) may be masked by layover effects, due to an insufficient spatial resolution with respect to forest height which governs the combined effects of shadowing and backscatter reinforcement at the front edge of the clearing (Fig. 7). Although surprising, these results highlight the importance of vegetation surrounding disturbed forest patches. Structure and height have an important impact on C-band detection capability and are a determinant of the disturbance itself. One should notice that simulations were made for single images (as opposed to time series) acquired at 35° elevation angle, the Sentinel-1 acquisition scenario. Stepper or more grazing local incidence angle would significantly change the results. Simulations also suggested that more subtle effects such as selective logging or thinning may not be easily detected using C- or L-band from single or temporally sparse acquisitions. The longer P-band wavelength was better suited for retrieving small intensity forest disturbances (Fig. 8). P-band SAR data from the future BIOMASS mission may provide the information needed to monitor low intensity forest disturbances although the reduced lifespan (five years), biannual revisit, relatively low spatial resolution (60m) and radio frequency interferences may prevent its utility under a time-critical operational scenario. Therefore, additional research effort is needed to overcome the limitations exposed for C-band. For example, research into more advanced techniques exploiting the dense time series available from Sentinel-1 mission as well as combining acquisition from both ascending and descending passes. Although such efforts are underway (Belenguer-Plomer et al., 2018; Bouvet et al., 2018; Reiche et al., 2018) specific algorithms adapted to Romanian forests may be needed as steep topography, small areas affected and low intensity degradation (e.g. selective logging) imply significant challenges not encountered in regions characterized by flat terrain and degradation-deforestation processes over much larger forest patches.

5. Conclusions

This study analyzed the potential of using the C-, L- and P-band SAR detests to monitor and retrieve the forest characteristics of interest (e.g., condition, disturbance) for an operational Romanian forest monitoring system that integrates in situ with and Earth-Observation datasets. According to the local forest monitoring needs, the requirements for such a system are i) high spatial resolution (<50 m) to resolve forest heterogeneity caused by the generally steep orography and divergent management practices, ii) high temporal resolution to allow near-real-time monitoring of frequent changes (e.g. canopy defoliation), deforestation and forest degradation and iii) reliable estimation for specific indicators on a frequent basis. Only few SAR satellite missions fulfill such conditions, ESA`s Sentinel and to a lesser extent JAXA`s PALSAR (due to the relatively low revisit time and access restrictions).

SAR utility for forest monitoring activities were studied through the Multistatic Polarimetric Interferometric Electromagnetic model for Remote Sensing (MIPERS^{4D}) simulation model. MIPERS^{4D} simulations were parameterized with information collected over 2017-2018 vegetation seasons within representative stands from the main forest species in Romania. The simulations were focused on the sensitivity of SAR to changes in three core parameters, namely vegetation water content, leaf area index and forest disturbance that may significantly impact radar scattering from forested areas. C-band simulations were of particular interest since operational monitoring systems need access to systematic satellite data collected with consistent acquisition modes over long periods.

The results confirmed quantitatively the differentiated sensitivity, to the three core parameters, as a function of SAR wavelength and forest structure with the least sensitive wavelength being the C-band. L- and P-band varied significantly with stand age particularly for the cross-polarized backscatter. However, C-band backscatter coefficient was sensitive to foliage volume, due to the increased attenuation, indicating potential for monitoring changes at canopy level (e.g. defoliation). C-band sensitivity to clear-cuts can be easily masked by the combined effect of shadowing and backscatter reinforcement at the front edge of the clearing, which demonstrate the importance of spatial resolution and filtering. Simulations also suggested that subtle effects (e.g. selective logging, thinning) may not be easily detected using C- or L-band data when temporally sparse acquisitions are available. Conversely, P-band was better suited for retrieving small intensity forest disturbance.

This study exposed the strengths and shortcomings of currently available spaceborne SAR wavelengths in the context of forest monitoring activities and highlighted the need for developing novel processing and modeling techniques based on dense time-series from satellite multi-frequency radar constellations. Combining multifrequency SAR data at P, L and C-band may constitute a key advancement towards the development of retrieval methods to characterize forest changes at regional or country levels. Passive (e.g. optical) sensors may provide the additional information needed to monitor and characterize forest changes within an operational context that responds to the Romanian commitments under the Ministerial Conference on the Protection of Forest in Europe, the Kyoto Protocol and the Convention on Biological Diversity.

Acknowledgments

This study was conducted under the project “Prototyping an Earth-Observation based monitoring and forecasting system for the Romanian forests” (EO-ROFORMON, project ID P_37_651/105058) funded by the Romanian National Authority for Scientific Research and Innovation and the European Regional Development Fund. We also acknowledge contributions to the project experimental design from Dr. Thuy le Toan, Dr. Maurizio Santoro and Dr. Robert Kennedy.

References

Alivernini A, Fares S, Ferrara C, Chianucci F. An objective image analysis method for estimation of canopy attributes from digital cover photography. Trees 2018; 32: 713-723.

Anfodillo T, Carrer M, Valle ED, Giacoma E, Lamedica S, Pettenella D. Current State of Forest Resources in the Carpathians. Activity 2.7: Forestry and timber industry. In: Legnaro: Università Degli Studi Di Padova DTeSA-F, editor, 2008.

Askne JIH, Santoro M, Smith G, Fransson JES. Multitemporal Repeat-Pass SAR Interferometry of Boreal Forests. IEEE Transactions on Geoscience and Remote Sensing 2003; 41: 1540-1550.

Asner GP, Scurlock JMO, Hicke JA. Global synthesis of leaf area index observations: implications for ecological and remote sensing studies. Global Ecology and Biogeography 2003; 12: 191-205.

Baccini A, Laporte N, Goetz SJ, Sun M, Dong H. A first map of tropical Africa’s above-ground biomass derived from satellite imagery. Environmental Research Letters 2008; 3: 1-9.

Belenguer-Plomer MA, Tanase MA, Fernandez-Carrillo A, Chuvieco E. Insights into burned areas detection from Sentinel-1 data and locally adaptive algorithms. Vol 10788: SPIE, 2018.

Bouvet A, Mermoz S, Ballère M, Koleck T, Toan TL. Use of the SAR Shadowing Effect for Deforestation Detection with Sentinel-1 Time Series. Remote Sensing 2018; 10.

Bruschi P, Vendramin GG, Bussotti F, Grossoni P. Morphological and Molecular Diversity Among Italian Populations of Quercus petraea (Fagaceae). Annals of Botany 2003; 91: 707-716.

Bussotti F, Pancrazi M, Matteucci G, Gerosa G. Leaf morphology and chemistry in Fagus sylvatica (beech) trees as affected by site factors and ozone: results from CONECOFOR permanent monitoring plots in Italy. Tree Physiology 2005; 25: 211-219.

Daily GC. Nature's Services. Washington D.C: Island Press, 1997.

Dale VH, Joyce S, McNulty RP, Neilson MP, Ayres MD, Flannigan PJ, et al. Climate Change and Forest Disturbances. BioScience 2001; 51: 723.

DeFries R, Achard F, Brown S, Herold M, Murdiyarso D, Schlamadinger B, et al. Earth observations for estimating greenhouse gas emissions from deforestation in developing countries. Environmental Science and Policy 2007 10: 385-394.

García-Martín A, Pérez-Cabello F, Fernández JdlR, Llovería RM. Estimation of Crown Biomass of Pinus spp. From Landsat TM and Its Effect on Burn Severity in a Spanish Fire Scar. IEEE Journal of Selected Topics in Applied Earth Observation and Remote Sensing 2008; 1: 254-265.

Garestier F, Dubois-Fernandez PC, Papathanassiou KP. Pine Forest Height Inversion Using Single-Pass X-Band PolInSAR Data. IEEE Transactions on Geoscience and Remote Sensing 2008; 46: 59-68.

Gazol A, Julio Camarero J, Gutierrez E, Popa I, Andreu-Hayles L, Motta R, et al. Distinct effects of climate warming on populations of silver fir (Abies alba) across Europe. Journal of Biogeography 2015; 42: 1150-1162.

Griffiths P, Kuemmerle T, Kennedy RE, Abrudan IV, Knorn J, Hostert P. Using annual time-series of Landsat images to assess the effects of forest restitution in post-socialist Romania. Remote Sensing of Environment 2012; 118: 199-214.

Hamadi A, Villard L, Borderies P, Albinet C, Koleck T, Toan TL. Comparative Analysis of Temporal Decorrelation at P-Band and Low L-Band Frequencies Using a Tower-Based Scatterometer Over a Tropical Forest. IEEE Transactions on Geoscience and Remote Sensing Letters 2017; 14: 1918-1922.

Hansen MC, Potapov PV, Moore R, Hancher M, Turubanova S, Tyukavina A, et al. High-resolution global maps of 21st-century forest cover change. science 2013; 342: 850-853.

Hansen MC, S. dR, Townshend JRG, M. C, C. D, A. SR. Global Percent Tree Cover at a Spatial Resolution of 500 Meters: First Results of the MODIS Vegetation Continuous Fields Algorithm. Earth Interactions 2003; 7: 1087-3562.

Hédl R, Svátek M, Dancák M, A.W. R, A.B. MS, A.S. K. A new technique for inventory of permanent plots in tropical forests: a case study from lowland dipterocarp forest in Kuala Belalong, Brunei Darussalam. 2009.

Hill J, Stellmes M, Stoffels J, Werner W, Frantz D, Stern O. Assesing the sensitivity of the European beech (Fagus sylvatica L.) to drought stress based on remote sensing measurements from earht observation satellite. 1st EARSeL Workshop on Operational Remote Sensing in Forest Management. EARSEL, Prague, Czech Republic, 2011, pp. 1-9.

Jenkins J, Kicklighter D, Aber J. Regional Impacts of Climate Change and Elevated Carbon Dioxide on Forest Productivity. In: Mickler R, Birdsey R, Hom J, editors. Responses of Northern U.S. Forests to Environmental Change. 139. Springer New York, 2000, pp. 383-423.

Karlson M, Ostwald M, Reese H, Sanou J, Tankoano B, Mattsson E. Mapping Tree Canopy Cover and Aboveground Biomass in Sudano-Sahelian Woodlands Using Landsat 8 and Random Forest. Remote Sensing 2015; 7: 10017-10041.

Knorn J, Kuemmerle T, Radeloff VC, Szabo A, Mindrescu M, Keeton WS, et al. Forest restitution and protected area effectiveness in post-socialist Romania. Biological Conservation 2012; 146: 204-212.

Lange H, Solberg S. Leaf area index estimation using LIDAR and forest reflectance modelling of airborne hyperspectral data. In: International I, editor. Geoscience and Remote Sensing Symposium, 2008. IGARSS 2008. 3. IEEE, Boston, 2008, pp. 475-478.

Laurin GV, Puletti N, WilliamHawthorne, Liesenberg V, Corona P, Papale D, et al. Discrimination of tropical forest types, dominant species, and mapping of functional guilds by hyperspectral and simulated multispectral Sentinel-2 data. Remote Sensing of Environment 2016; 176: 163-176.

Le Toan T, Beaudoin A, Guyon D. Relating forest biomass to SAR data. IEEE Transactions on Geoscience and Remote Sensing 1992; 30: 403-411.

Lefsky MA. A global forest canopy height map from the Moderate Resolution Imaging Spectroradiometer and the Geoscience Laser Altimeter System. Geophysical Research Letters 2010; 37: L15401.

Lewis AJ, Henderson FM. Radar Fundamentals: The Geoscience perspective. In: Henderson FM, Lewis AJ, editors. Principles and Applications of Imaging Radar. 2. John Wiley & Sons, 1999, pp. 866.

Lohberger S, St€angel M, Atwood EC, Siegert F. Spatial evaluation of Indonesia’s 2015 fire-affected area and estimated carbon emissions using Sentinel-1. Global Change Biology 2017.

Lucas R, Armston J, Fairfax R, Fensham R, Accad A, Carreiras J, et al. An Evaluation of the ALOS PALSAR L-Band Backscatter - Above Ground Biomass Relationship Queensland, Australia: Impacts of Surface Moisture Condition and Vegetation Structure. IEEE Journal of Selected Topics in Applied Earth Observation and Remote Sensing 2010; 3: 576-593.

McDonald KC, Zimmermann R, Kimball JS. Diurnal and Spatial Variation of Xylem Dielectric Constant in Norway Spruce (Picea abies [L.] Karst.) as Related to Microclimate, Xylem Sap Flow, and Xylem Chemistry. IEEE Transactions on Geoscience and Remote Sensing 2002; 40: 2063-2082.

McNicol IM, Ryan CM, Mitchard ETA. Carbon losses from deforestation and widespread degradation offset by extensive growth in African woodlands. Nature Communications 2018; 9.

Mermoz S, Le Toan T. Forest Disturbances and Regrowth Assessment Using ALOS PALSAR Data from 2007 to 2010 in Vietnam, Cambodia and Lao PDR. Remote Sensing 2016; 8: 2072-4292.

Michel A, Seidling W. Forest Condition in Europe. 2014 Technical Report of ICP Forests. Report under the UNECE Convention on Long-Range Transboundary Air Pollution (CLRTAP). In: Michel A, Seidling W, editors. BFW-Dokumentation 18/2014. BFW Austrian Research Centre for Forests, Vienna, 2014, pp. 1-164.

Michelakis D, Stuart N, Lopez G, Linares V, Woodhouse IH. Local-Scale Mapping of Biomass in Tropical Lowland Pine Savannas Using ALOS PALSAR. Forests 2014; 5: 2377-2399.

Mitchard E, Saatchi SS, Lewis SL, Feldpausch TR, Gerard FF, Woodhouse IH, et al. Comment on ‘A first map of tropical Africa’s above-ground biomass derived from satellite imagery. Environmental Research Letters 2011a; 6: 1-6.

Mitchard ETA. The tropical forest carbon cycle and climate change. Nature 2018; 559: 527-534.

Mitchard ETA, Saatchi SS, White LJT, Abernethy KA, Jeffery KJ, Lewis SL, et al. Mapping tropical forest biomass with radar and spaceborne LiDAR in Lope National Park, Gabon: overcoming problems of high biomass and persistent cloud. Biogeosceinces 2011b; 9: 179-191.

Neumann M, Saatchi SS, Ulander LMH, Fransson JES. Assessing Performance of L- and P-Band Polarimetric Interferometric SAR Data in Estimating Boreal Forest Above-Ground Biomass. IEEE Transactions on Geoscience and Remote Sensing 2012; 50: 714-726.

Nielsen MM, Heurich M, Malmberg B, Brun A. Automatic Mapping of Standing Dead Trees after an Insect Outbreak Using the Window Independent Context Segmentation Method. Journal of Forestry 2014; 112: 564-571.

Niinemets U. Acclimation to low irradiance inPicea abies: influences of past and present light climate on foliage structure and function. Tree Physiology 1997; 17: 723-732.

Obersteiner M, Böttcher H, Yamagata Y. Terrestrial ecosystem management for climate change mitigation. Current Opinion in Environmental Sustainability 2010; 2: 271-276.

Ojea E, Nunes PALD, Loureiro ML. Mapping Biodiversity Indicators and Assessing Biodiversity Values in Global Forests. Environmental and Resource Economics 2010; 47: 329-347.

Olson DM, Dinerstein E, Wikramanayake ED, Burgess ND, Powell GVN, Underwood EC, et al. Terrestrial Ecoregions of the World: A New Map of Life on Earth: A new global map of terrestrial ecoregions provides an innovative tool for conserving biodiversity. BioScience 2001; 51: 933-938.

Petritan AM, Lupke Bv, Petritan IC. A comparative analysis of foliar chemical composition and leaf construction costs of beech (Fagus sylvatica L.), sycamore maple (Acer pseudoplatanus L.) and ash (Fraxinus excelsior L.) saplings along a light gradient. Annals of Forest Science 2010; 67: 610.

Popa I. Windthrow risk management. Results from Romanian forests. Forest Disturbances and Effects on Carbon Stock: The Non-Permanence Issue, San Vito di Cadore, 2008.

Potapov PV, Turubanova SA, Tyukavina A, Krylov AM, McCart JL, Radeloff VC, et al. Eastern Europe's forest cover dynamics from 1985 to 2012 quantified from the full Landsat archive. Remote Sensing of Environment 2015; 159: 28-43.

Poulter B, Cadule P, Cheiney A, Ciais P, Hodson E, Peylin P, et al. Sensitivity of global terrestrial carbon cycle dynamics to variability in satellite-observed burned area. Global Biogeochemical Cycles 2015; 29: 207-222.

Reiche J, Hamunyela E, Verbesselt J, Hoekman D, Herold M. Improving near-real time deforestation monitoring in tropical dry forests by combining dense Sentinel-1 time series with Landsat and ALOS-2 PALSAR-2. Remote Sensing of Environment 2018; 204: 147-161.

Rodríguez-Veiga P, Saatchi S, Tansey K, Balzter H. Magnitude, spatial distribution and uncertainty of forest biomass stocks in Mexico. Remote Sensing of Environment 2016; 183: 265-281.

Rullan-Silva CD, Olthoff AE, Mata JADdl, Pajares-Alonso JA. Remote monitoring of forest insect defoliation. A review. Forest Systems 2013; 22: 377-391.

Saatchi SS, Harris NL, Brown S, Lefsky M, Mitchard ETA, Salas W, et al. Benchmark map of forest carbon stocks in tropical regions across three continents. PNAS 2011; 108: 9899-9904.

Salberg AB, Solberg S, Weydahl DJ, Astrup R. Leaf Area Index Estimation Using ENVISAT ASAR and Radarsat-2. In: Center NC, editor, SAMBA/30/09, 2009.

Sandberg G, Ulander LMH, Fransson JES, Holmgren J, Toan TL. L- and P-band backscatter intensity for biomass retrieval in hemiboreal forest. Remote Sensing of Environment 2011; 115: 2874-2886.

Santoro M, Pantze A, Fransson JES, Dahlgren J, Persson A. Nation-Wide Clear-Cut Mapping in Sweden Using ALOS PALSAR Strip Images. Remote Sensing 2012; 4: 1693-1715.

Saxe H, Cannell MGR, Johnsen Ø, Ryan MG, Vourlitis G. Tree and forest functioning in response to global warming. New Phytologist 2001; 149: 369-399.

Schaich H, Milad M. Forest biodiversity in a changing climate: which logic for conservation strategies? Biodiversity and Conservation 2013; 22: 1107-1114.

Scheller RM, Mladenoff DJ. A spatially interactive simulation of climate change, harvesting, wind, and tree species migration and projected changes to forest composition and biomass in northern Wisconsin, USA. Global Change Biology 2005; 11: 307-321.

Schimel D, Melillo J, Tian H, McGuire AD, Kicklighter D, Kittel T, et al. Contribution of increasing CO2 and climate to carbon storage by ecosystems in the United States. Science 2000; 287: 2004-6.

Seidl R, Schelhaas MJ, Rammer W, Verkerk PJ. Increasing forest disturbances in Europe and their impact on carbon storage. Nature Climate Change 2014; 4: 806-810.

Senf C, Seidl R, Hostert P. Remote sensing of forest insect disturbances: current state and future directions. International Journal of Applied Earth Observation and Geoinformation 2017; in press.

Shimada M, Itoh T, Motooka T, Watanabe M, Shiraishi T, Thapa R, et al. New global forest/non-forest maps from ALOS PALSAR data (2007–2010). Remote Sensing of Environment 2014; 155: 13-31.

Simard M, Pinto N, Fisher JB, Baccini A. Mapping forest canopy height globally with spaceborne lidar. Journal of Geophysical Research 2011; 116: 1-12.

Solberg S. Mapping gap fraction, LAI and defoliation using various ALS penetration variables. International Journal of Remote Sensing 2010; 31: 1227-1244.

Solberg S, Astrup R, Weydahl DJ. Detection of Forest Clear-Cuts with Shuttle Radar Topography Mission (SRTM) and Tandem-X InSAR Data. Remote Sensing 2013; 5: 5449-5462.

Spruce JP, Sader S, Ryan RE, Smoot J, Kupe P, Ross K, et al. Assessment of MODIS NDVI time series data products for detecting forest defoliation by gypsy moth outbreaks. Remote Sensing of Environment 2011; 115: 427-437.

Steffen KT, Cajthaml T, Snajdr J, Baldrian P. Differential degradation of oak (Quercus petraea) leaf litter by litter-decomposing basidiomycetes. Research in Microbiology 2007; 158: 447-455.

Stojnić S, Orlović S, Miljkovic D, Wuehlisch Gv. Intra- and interprovenance variations in leaf morphometric traits in European beech (Fagus sylvatica L.). Archives of Biological Sciences 2016; 68: 781-788.

Tanase M, de la Riva J, Santoro M, P\'e r-C, Fernando, Kasischke E. Sensitivity of SAR data to post-fire forest regrowth in Mediterranean and boreal forests. Remote Sensing of Environment 2011a; 115: 2075-2085.

Tanase M, Ismail I, Lowell K, Karyanto O, Santoro M. Detecting and quantifying forest change: the potential of existing C- and X-band radar datase. PLOS ONE 2015a; 10(6): e0131079: 1-14.

Tanase MA, Aponte C, Mermoz S, Bouvet A, Le Toan T, Heurich M. Detection of windthrows and insect outbreaks by L-band SAR: A case study in the Bavarian Forest National Park. Remote Sensing of Environment 2018; 209: 700-711.

Tanase MA, de la Riva J, Santoro M, Pérez-Cabello F, Kasischke E. Sensitivity of SAR data to post-fire forest regrowth in Mediterranean and boreal forests. Remote Sensing of Environment 2011b; 115: 2075-2085.

Tanase MA, Kennedy R, Aponte C. Radar Burn Ratio for fire severity estimation at canopy level: An example for temperate forests. Remote Sensing of Environment 2015b; 170: 14-31.

Tanase MA, Panciera R, Lowell K, Aponte C, Hacker JM, Walker JP. Forest Biomass Estimation at High Spatial Resolution: Radar vs. Lidar sensors. IEEE Transactions on Geoscience and Remote Sensing Letters 2014; 11: 711-715.

Tropek R, Sedláček O, Beck J, Keil P, Musilová Z, Šímová I, et al. Comment on “High-resolution global maps of 21st-century forest cover change”. Science 2018; 344: 1-4.

Verbyla DL, Kasischke ES, Hoy EE. Seasonal and topographic effects on estimating fire severity from Landsat TM/ETM+ data International Journal of Wildland Fire 2008; 17: 527-534.

Villard L. Forward and inverse modeling of synthetic aperture radar in the bistatic configuration: Applications in forest remote sensing. ONERA-ISAE. PhD. Paul-Sabatier, Toulouse, 2009.

Villard L, Le Toan T, Ho Tong Minh D, Mermoz S, Bouvet A. Forest Biomass From Radar Remote Sensing. In: Zribi M, editor. Land Surface Remote Sensing in Agriculture and Forest. Elsevier, 2016, pp. 363-425.

Wang WM, Li ZL, Su HB. Comparison of leaf angle distribution functions: Effects on extinction coefficient and fraction of sunlit foliage. Agricultural and Forest Meteorology 2007; 143: 106-122.

Zhao Y, Zeng Y, Zhen Z, Dong W, Zhao D, Wu B, et al. Forest species diversity mapping using airborne LiDAR and hyperspectral data in a subtropical forest in China. Remote Sensing of Environment 2018; 213: 104-114.